



## Exposure to TiO<sub>2</sub> nanoparticles induces shifts in the microbiota composition of *Mytilus galloprovincialis* hemolymph



Manon Auguste<sup>a,\*</sup>, Aide Lasa<sup>a,b,1</sup>, Alberto Pallavicini<sup>c</sup>, Stefano Gualdi<sup>d</sup>, Luigi Vezzulli<sup>a</sup>, Laura Canesi<sup>a</sup>

<sup>a</sup> DISTAV, Dept. of Environmental, Earth and Life Sciences, University of Genoa, Italy

<sup>b</sup> Department of Microbiology and Parasitology, Universidade de Santiago de Compostela, Santiago de Compostela, Spain

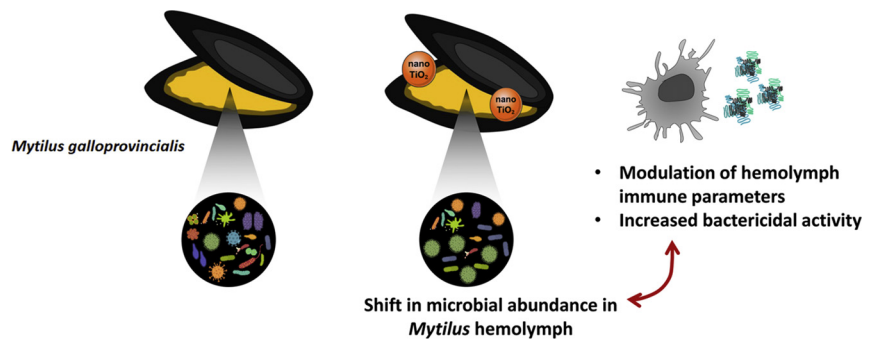
<sup>c</sup> Dept. of Life Sciences, University of Trieste, Italy

<sup>d</sup> Department of Plant and Microbial Biology, University of Zürich, Switzerland

### HIGHLIGHTS

- Potential impact of NPs on the microbiome of marine organisms
- nTiO<sub>2</sub> exposure affected microbiota composition of *Mytilus* hemolymph.
- nTiO<sub>2</sub> also affects immune hemolymph parameters.
- Interconnection between microbial communities and immune system of bivalve host

### GRAPHICAL ABSTRACT



### ARTICLE INFO

#### Article history:

Received 31 January 2019

Received in revised form 7 March 2019

Accepted 9 March 2019

Available online 14 March 2019

Editor: Henner Hollert

#### Keywords:

TiO<sub>2</sub> nanoparticles

*Mytilus*

Hemolymph

Microbiota

16S rRNA

Innate immunity

### ABSTRACT

It is now recognized that host microbiome, the community of microorganisms that colonize the animal body (e.g. microbiota) and their genomes, play an important role in the health status of all organisms, from nutrient processing to protection from disease. In particular, the complex, bilateral interactions between the host innate immune system and the microbiota are crucial in maintaining whole body homeostasis.

The development of nanotechnology is raising concern on the potential impact of nanoparticles-NPs on human and environmental health. Titanium dioxide-nTiO<sub>2</sub>, one of the most widely NP in use, has been shown to affect the gut microbiota of mammals and fish, as well as to potentially alter microbial communities. In the marine bivalve *Mytilus galloprovincialis*, nTiO<sub>2</sub> has been previously shown to interact with hemolymph components, thus resulting in immunomodulation. However, no information is available on the possible impact of NPs on the microbiome of marine organisms.

Bivalves host high microbial abundance and diversity, and alteration of their microbiota, in both tissues and hemolymph, in response to stressful conditions has been linked to a compromised health status and susceptibility to diseases. In this work, the effects of nTiO<sub>2</sub> exposure (100 µg/L, 4 days) on *Mytilus* hemolymph microbiota were investigated by 16S rRNA gene-based profiling. Immune parameters were also evaluated. Although hemolymph microbiota of control and nTiO<sub>2</sub>-treated mussels revealed a similar core composition, nTiO<sub>2</sub> exposure affected the abundance of different genera, with decreases in some (e.g. *Shewanella*, *Kistimonas*, *Vibrio*) and increases in others (e.g. *Stenotrophomonas*). The immunomodulatory effects of nTiO<sub>2</sub> were confirmed by the increase in the bactericidal activity of whole hemolymph. These represent the first data on the effects of NPs on the microbiome

\* Corresponding author at: DISTAV, University of Genoa, Palazzo delle Scienze 26, 16132 Genoa, Italy.

E-mail address: [manon.auguste@edu.unige.it](mailto:manon.auguste@edu.unige.it) (M. Auguste).

<sup>1</sup> Equally contributed to the manuscript.

of marine invertebrates, and suggest that the shift in hemolymph microbiome composition induced by nTiO<sub>2</sub> may result from the interplay between the microbiota and the immune system.

© 2019 The Authors. Published by Elsevier B.V. This is an open access article under the CC BY-NC-ND license (<http://creativecommons.org/licenses/by-nc-nd/4.0/>).

## 1. Introduction

The impact of microbiota, the community of microorganisms that colonize the animal body on immune homeostasis within the gut and, importantly, also at systemic sites, has gained tremendous research interest over the last few years (Pflughoft and Versalovic, 2012; Shreiner et al., 2015; Thaïss et al., 2016). From human studies, it is now recognized that host microbiota play an important role in the health status of all animals, from nutrient processing to protection from diseases (Brugman et al., 2018; Flandroy et al., 2018; Ikeda-Ohtsubo et al., 2018).

Marine invertebrates host high microbial abundance and diversity (Olson and Kellogg, 2010), and alteration of their microbiota due to stressful conditions and/or environmental changes has been linked with a condition of a compromised health status and susceptibility to diseases (Bourne et al., 2016; Pita et al., 2018).

Bivalve molluscs may be considered pertinent animal models for studying host-microbiota interactions since, through their filter-feeding habit they face large numbers of microorganisms. In particular, increasing mass mortality episodes of the pacific oyster (*Crassostrea gigas*) in farming areas are attributed to complex interactions among oysters, their microbiota and environmental variables (Pernet et al., 2014; de Lorgeril et al., 2018; Green et al., 2018; Khan et al., 2018; King et al., 2018). Furthermore, the well accepted presence of microorganisms in the hemolymph of healthy bivalves indicates that this ecosystem could shield and limit settlement of pathogenic strains (Desriac et al., 2014), and release antimicrobial compounds that potentially play a role in the control of microbial community and health recovery (Defer et al., 2013), thus contributing to host homeostasis. The hemolymph associated microbiota has been investigated in oysters in response to pathogens (Wendling et al., 2014) and to temperature stress and infection (Lokmer and Mathias Wegner, 2015; Pierce and Ward, 2018). In contrast, information is scarce in other species of widely farmed bivalves such as *Mytilus* spp., that are generally not affected by mortality events, being less sensitive to changes in environmental conditions and microbial infection. Microbiota profiles have been recently evaluated in hemolymph and digestive gland of the Mediterranean mussel *M. galloprovincialis* (Vezzulli et al., 2017).

The recent expansion of nanotechnology has led to increasing concern on the potential consequences of exposure to nanoparticles (NPs) for human and environmental health. Many nano-oxides (such as nTiO<sub>2</sub>, nSiO<sub>2</sub>, nZnO) are currently added to a variety of consumer products including food, thus attracting interest on the potential effects of NPs on mammalian gut microbiota (Pietrojusti et al., 2016; Dufefoi et al., 2017; Bouwmeester et al., 2018). Titanium dioxide (nTiO<sub>2</sub>) is one of the most widely NP in production and use (Robichaud et al., 2009). As a food additive, TiO<sub>2</sub> (referred to as E171, EFSA, 2016), can contain up 44% nanosized TiO<sub>2</sub> (Dufefoi et al., 2017 and references quoted therein). In mice, oral administration of nTiO<sub>2</sub> affects the gastrointestinal tract and gut microbiota (J. Li et al., 2018). In pregnant rats, nTiO<sub>2</sub> induced the alteration of gut microbiota and increased the fasting blood glucose (Mao et al., 2019).

The direct antimicrobial functions of nTiO<sub>2</sub> have been widely demonstrated: exposure to high concentrations of nTiO<sub>2</sub> (in the range of mg-g/L) reduces bacterial growth (Foster et al., 2011; Maurer-Jones et al., 2013; Ananpattarachai et al., 2016; Vimbela et al., 2017). Similarly, high concentrations of nTiO<sub>2</sub> can potentially alter the composition of planktonic and sessile bacterial communities (Binh et al., 2014; Jomini et al., 2015). In the zebrafish, chronic exposure to nTiO<sub>2</sub> induced changes in microbiome composition and altered physiological functions

(Chen et al., 2018). Although these data suggest that a possible impact of nTiO<sub>2</sub> on aquatic microbiota, no information is available in marine species. In the marine environment, predicted environmental concentrations of nTiO<sub>2</sub> range from ng/L to µg/Kg in surface waters and sediments, respectively. However, due to its massive use, environmental levels of nTiO<sub>2</sub> are likely to increase and to be unequally distributed (Menard et al., 2011; Gottschalk et al., 2015), with coastal zones possibly more impacted by NPs (Haynes et al., 2017). Therefore, exposure to nTiO<sub>2</sub> may also affect the microbiota of marine invertebrates, including mussels.

In *M. galloprovincialis*, the effects of nTiO<sub>2</sub> have been thoroughly investigated both in vitro and in vivo, revealing multiple responses from molecular to organism level; in particular nTiO<sub>2</sub> has been shown to affect several immune parameters in both circulating hemocytes and hemolymph serum, resulting in immunomodulation (Barmo et al., 2013; Canesi and Procházková, 2013; Balbi et al., 2014; Corsi et al., 2014; Canesi et al., 2016; Canesi and Corsi, 2016). In this work, the effects of nTiO<sub>2</sub> on mussel hemolymph microbiome were investigated through targeted high-throughput sequencing of the 16S rRNA gene (V4 hyper-variable region) using Ion Torrent sequencing technology. Exposure conditions (100 µg/L, 96 h) were chosen on the basis of the most extensive data previously obtained not only on nTiO<sub>2</sub>-induced immunomodulation, but also on functional and molecular responses and accumulation at the tissue level (Barmo et al., 2013; Balbi et al., 2014; Della Torre et al., 2015).

## 2. Materials and methods

### 2.1. Characterization of nTiO<sub>2</sub>

The nanosized Titanium Dioxide (nTiO<sub>2</sub>) used within this study (commercial Aeroxide® P25 Titanium Dioxide powder, declared particle size: 21 nm) provided from Degussa Evonik (Essen, Germany), has been thoroughly characterized for the physico-chemical properties of primary particles (Ciacci et al., 2012; Brunelli et al., 2013) and behavior in exposure media (artificial sea water-ASW) (Barmo et al., 2013; Brunelli et al., 2013; Balbi et al., 2014). Mean average size and shape of primary particles were determined by Transmission Electron Microscope (TEM) analysis on a Jeol (Tokyo, Japan) 3010 transmission electron microscope operating at 300 kV. Surface area and pore volume were obtained by the method of Brunauer, Emmett and Teller (BET) by nitrogen adsorption on a Micrometrics ASAP2000 Accelerated Surface Area and Porosimetry System at an adsorption temperature of −196 °C, after pretreating the sample under high vacuum at 300 °C for 2 h. nTiO<sub>2</sub> behavior in ASW was determined by Dynamic Light Scattering-DLS analysis. For further details, see references above.

### 2.2. Mussel collection and hemolymph sampling

Mussels (*Mytilus galloprovincialis* Lam.), 5–6 cm long, were purchased in November 2017 from a shellfish farm located in the Gulf of La Spezia (Ligurian Sea, Italy), the main shellfish production area in northwestern Italy, after 24 h depuration by ozonization according to the Italian and European laws. Mussels were transferred to the laboratory, cleaned of epibionts, repeatedly washed (three times) with artificial sea water-ASW to remove part of the external non-resident microbiota, and acclimatized for 24 h in static tanks containing aerated ASW (ASTM, 2004), pH 7.9–8.1, 36 ppt salinity (1 L/animal), at 16 ± 1 °C.

Mussels (20 animals) were exposed 96 h to nTiO<sub>2</sub> at the concentration 100 µg/L/animal as previously described (Barmo et al., 2013; Balbi et al., 2014). nTiO<sub>2</sub> suspensions were prepared using 15 mg of pristine powder suspended in 3 mL milliQ water, then sonicated using a probe sonication for 15 min in an ice bath with a UP200S Hielscher Ultrasonic Technology (Teltow, Germany) at 100 W, 50% on/off cycle, and immediately spiked in the tanks in order to reach the desired nominal concentration. A parallel group of control (untreated) mussels were kept in clean ASW. Animals were not fed during the experiments. Sea water was changed daily before addition of nTiO<sub>2</sub>. No mortality was observed in different experimental conditions.

After 96 h, hemolymph was extracted from the adductor muscle of 4 animals for each condition (C1–C4 = control mussels; T1–T4 = nTiO<sub>2</sub> exposed mussels), using a sterile syringe with an 18 G1/2" needle, filtered with gauze, at 16 °C. Aliquots of 200 µL from each individual were utilized for microbiome analysis.

Moreover, aliquots of hemolymph (pooled from 10 to 12 animals) were utilized for evaluation of immune parameters: lysosomal membrane stability (LMS) on hemocytes, lysozyme activity in hemolymph serum, and bactericidal activity of whole hemolymph samples.

Aliquots (1 L) of exposure medium, 1 replicate per condition (seawater from control-CW and nTiO<sub>2</sub> exposure-TW) were sampled and directly filtered on 0.2 µm Nucleopore filters (45 mm). All samples were frozen at –20 °C until further analysis.

### 2.3. Preparation of DNA library and sequencing

#### 2.3.1. Sampling and DNA extraction

DNA was extracted from aliquot of 200 µL of whole hemolymph of control and nTiO<sub>2</sub>-exposed mussels using High Pure PCR Template Preparation Kit (Roche Diagnostics), according to the manufacturer's instructions and as previously described (Vezzulli et al., 2017). For water samples, 1 L of seawater was filtered on 0.2 µm Nucleopore filters (45 mm) and DNA was extracted with the PowerWater DNA Isolation Kit (Mo Bio laboratories, inc), following the manufacturer's instructions. The amount of DNA extracted was determined fluorimetrically with QuantiFluor™ dsDNA System using a QuantiFluor™ fluorometer (Promega Italia srl, Milano, Italy).

#### 2.3.2. 16S rRNA gene amplification and sequencing

16S rRNA PCR amplicon libraries were generated from genomic DNA extracted from bivalve samples using primers amplifying the V4 hyper-variable region of the 16S rRNA gene of bacteria. All primers were custom designed to include 16SrRNA complementary regions (Table S1) plus the complementary sequences to the Ion Torrent specific adapters. Two PCR assays were performed. A first target enrichment PCR assay with the 16S conserved primers. A second PCR assay, with customised primers and included adapters' complementary regions. The obtained libraries were sequenced using an Ion Torrent (PGM) Platform. Bioinformatic analysis of NGS (Next Generation Sequencing) data was performed using the Microbial Genomics module (version 1.3) work-flow of the CLC Genomics workbench (version 9.5.1). The bioinformatic analysis of the data included a cleaning step of the reads (barcodes and primers removal), by trimming based on quality scores ( $Q < 30$ ) and length (100 base pairs-bp), as well as chimera detection and removal. Trimmed reads were clustered at 97% level of similarity into Operational Taxonomical Units (OTUs), that are defined as a cluster of sequences similarity which corresponds approximately to species level, and then classified against the non-redundant version of the SILVA SSU reference taxonomy database (release 119; <http://www.arb-silva.de>). Microbial diversity was also analysed in order to describe the diversity within a sample (Alpha-diversity) or between samples (Beta-diversity). Alpha-diversity index represents the species richness (number of taxa) within a single microbial environment, while Beta-diversity analyse the diversity in the microbial community between different environments. The Beta-diversity index is estimated between each pair of samples and,

based on the distance matrices calculated, a Principal Coordinates Analysis (PCoA) is performed. The core microbiome, defined as the OTUs present across all samples, was also analysed using the Corbata software (CORE microbiome Analysis Tools, (Li et al., 2013)).

### 2.4. Effects on hemolymph immune parameters

Hemocyte lysosomal membrane stability-LMS was evaluated by the NRR (Neutral Red Retention time) assay as previously described (Canesi et al., 2010, 2014; Barmo et al., 2013; Balbi et al., 2014). Hemocyte monolayers on glass slides were incubated with 20 µL of neutral red (NR) solution (final concentration 40 µg/mL from a stock solution of NR 40 mg/mL in DMSO); after 15 min excess dye was washed out and 20 µL of ASW was added. Every 15 min, slides were examined under an optical microscope and the percentage of cells showing loss of the dye from lysosomes in each field was evaluated. For each time point 10 fields were randomly observed, each containing 8–10 cells. The end point of the assay was defined as the time at which 50% of the cells showed sign of lysosomal leaking (the cytosol becoming red and the cells rounded). All incubations were carried out at 16 °C.

Serum lysozyme activity was evaluated as previously described (Balbi et al., 2014). To obtain hemolymph serum (i.e., hemolymph free of cells), whole hemolymph was centrifuged at 200 ×g for 10 min, and the supernatant was passed through a 0.22 µm filter. Lysozyme activity in aliquots of serum (control and exposed to nTiO<sub>2</sub>) was determined spectrophotometrically at 450 nm utilizing *Micrococcus lysodeikticus*. Hen eggwhite (HEW) lysozyme was used as a concentration reference and lysozyme activity was expressed as HEW lysozyme equivalents (U/mL/mg protein). Protein content was determined according to the bicinchoninic acid (BCA) method using bovine serum albumin (BSA) as a standard.

For the bactericidal assay, bacterial cultures (*Escherichia coli* strain MG1855) were prepared as previously described (Canesi et al., 2001). The *E. coli* suspension in phosphate buffered solution-PBS isotonic to hemolymph (PBS-NaCl: 0.1 M KH<sub>2</sub>PO<sub>4</sub>, 0.1 M Na<sub>2</sub>HPO<sub>4</sub>, 0.15 M NaCl; pH 7.2 to 7.4) was suitably diluted in aliquots (1 mL) of whole hemolymph samples obtained from Control and nTiO<sub>2</sub>-exposed mussels to yield a final bacteria/hemocyte ratio of approximately 50:1 (determined spectrophotometrically as an A<sub>650</sub> = 1, corresponding to 2–4 × 10<sup>9</sup> colony forming units [CFU]/mL). Incubations were carried out at 16 °C for 30 and 60 min in triplicate for each sampling time. Immediately after bacteria addition (T0) and after 30 and 60 min of incubation at 18 °C (T30 and T60), samples were lysed by adding 4.5 mL of cold distilled water followed by 10 min agitation. The collected hemocyte/bacteria lysates were ten-fold serial diluted in sterile ASW. Aliquots (100 µL) of the diluted samples were plated onto Luria-Bertani-LB agar (Scharlau, Spain) and the number of CFU/mL (representing cultivable bacteria which survived to hemocyte bactericidal activity) was determined after overnight incubation at 37 °C. Percentages of killing were then calculated as the ratio  $CFU_{T0} - CFU_T / CFU_{T0} \times 100$ . Data, representing the mean ± SD of at least four samples in triplicate, were analysed by Mann-Whitney *U* test. All statistical analysis were performed using the PRISM 7 GraphPad software.

## 3. Results

### 3.1. NPs characteristics and behavior in exposure medium

The nTiO<sub>2</sub> used within this study was previously characterized (Ciacci et al., 2012; Barmo et al., 2013; Brunelli et al., 2013; Balbi et al., 2014) and data are summarized in Table 1. Briefly, primary particles of uncoated nTiO<sub>2</sub> ranged from 10 to 65 nm size and showed an irregular shape (evaluated by TEM) and a surface area of 61 m<sup>2</sup>/g, as determined by BET method. The behavior of nTiO<sub>2</sub> in suspension in ASW (100 µg/L) was assessed by DLS analysis after 30 min, 25 h and 50 h. nTiO<sub>2</sub> showed a tendency to agglomeration, with the size of agglomerates increasing

**Table 1**  
Physico-chemical characterization of nTiO<sub>2</sub> primary particles and behavior in exposure medium (for experimental details see Barmo et al., 2013; Brunelli et al., 2013; Balbi et al., 2014). Upper panel: Primary particle characterization. Lower panel: Characterization of nTiO<sub>2</sub> suspensions in artificial seawater (ASW) (100 µg/L) over time (30 min, 25 and 50 h). Data are reported as mean ± SD.

nTiO <sub>2</sub> characterization	Crystal structure <sup>a</sup>	Shape <sup>a</sup>	Size distribution (nm) <sup>a</sup>	Surface area (m <sup>2</sup> /g) <sup>b</sup>	Pore size (mL/g) <sup>b</sup>	Surface chemistry <sup>c</sup>	Chemical composition <sup>a</sup>	Purity (%) <sup>d</sup>
nTiO <sub>2</sub> suspensions in ASW <sup>e</sup>	Anatase/rutile	Irregular	10–65	61	0.5	Uncoated	Ti, O	>99.5
	100 µg/L		30 min		25 h		50 h	
			180 ± 21		201 ± 26		304 ± 38	

<sup>a</sup> Determined by Transmission Electron Microscopy (TEM).

<sup>b</sup> Specific surface area calculated by the BET (Brunauer–Emmett–Teller) method.

<sup>c</sup> Declared by the supplier.

<sup>d</sup> Determined by Inductively Coupled Plasma Optical Emission Spectrometry (ICP-OES).

<sup>e</sup> Hydrodynamic size of nTiO<sub>2</sub> suspensions in ASW determined by Dynamic Light Scattering (DLS).

over time (from 180 ± 21 at 30 min to 304 ± 38 nm at 50 h). This type of nTiO<sub>2</sub> has been shown to retain a negative ζ-potential of about –10 mV in ASW over a 72 h period (Doyle et al., 2015).

### 3.2. Microbiota analysis

The microbiota was analysed in hemolymph samples from both control and nTiO<sub>2</sub>-exposed mussels. Moreover, to fully appreciate the dynamic exchange of microbes harbored in mussels with their surrounding media, the microbiota composition of seawater samples from each experimental condition was also investigated.

#### 3.2.1. General sequencing results

Sequencing of the 16S rRNA gene amplicons, targeting the V4 hyper-variable region from bacteria present in the hemolymph of mussels and seawater, produced a total of 871,022 reads. Raw sequences were trimmed and remaining sequences were first clustered at 97% similarity resulting in a total of 274,936 operational taxonomical units (OTUs) (Table S2). OTUs were BLASTed against SILVA reference database to estimate the taxonomic content of the data set, using SILVA taxonomy with the CLC software. Singletons (OTUs with a single read in the data set) were excluded from the analysis. As a result, 271,997 reads were assigned to the Bacteria domain while 2,939 remained unassigned. Rarefaction curves calculated for total OTUs abundance (Fig. 1) and Chao1 index (data not shown) reached the plateau, suggesting that sequencing depth was good enough to measure and compare diversity indexes among samples. Bias-corrected from of Chao 1 index calculated from 16S rRNA gene-based profiling analysis of the bacterial community in

seawater and *M. galloprovincialis* hemolymph was calculated, and no difference were observed among samples and treatments (data not shown).

#### 3.2.2. Microbial community composition in hemolymph of *M. galloprovincialis* and effect of nTiO<sub>2</sub> exposure

In all hemolymph samples, the microbial community composition included few OTUs accounting for the majority of the reads, with Proteobacteria (84.8%) and Bacteroidetes (12.5%) as the dominant phyla. These included Gammaproteobacteria (67.8%), Alphaproteobacteria (12.9%) and Flavobacteriia (10.8%) as the main classes across all samples.

The microbiome of hemolymph was investigated in control and nTiO<sub>2</sub>-exposed mussels and the results are presented in Fig. 2. In control samples, the bacterial community (Fig. 2A) appeared dominated by the genera *Stenotrophomonas* and *Kistimonas* (26.7 and 22.7% respectively), followed by other genera with lower relative abundances, namely *Shewanella* (5.5%), *Vibrio* (5.2%), *Psychrobium* (2.7%), *Polaribacter* (2.1%), *Amphritea* (1.7%), *Tenacibaculum* (1.5%), *Pseudoalteromonas* (1.3%) and *Arcobacter* (1.07%). When analysing the effects of nTiO<sub>2</sub> exposure, two distinct effects were observed. Increases in the relative abundance of some genera were observed with respect to controls, such as *Stenotrophomonas* (from 26.7% to 51.7%), *Variovorax* (from 0.7% to 2.6%), *Aquibacter* (from 0.6% to 1.6%) or *Sulfitobacter* (from 0.5% to 1.4%); in contrast, abundances of other genera were decreased after exposure, *Kistimonas* (from 22.7% to 0.002%), *Shewanella* (from 5.5% to 0.6%), *Vibrio* (from 5.2% to 0.5%), *Psychrobium* (from 2.7% to 0.2%) or *Arcobacter* (from 1.07% to 0.07%).

The core microbiome, which represent a set of microbes considered as stable community established within the host and constantly present among individuals, was investigated in hemolymph samples from both control and nTiO<sub>2</sub>-treated mussels (Fig. 2B). The results showed that in control samples the core microbiome was more diverse than that nTiO<sub>2</sub>-exposed samples when considering the same ubiquity and abundance threshold (e.g. 95% and 0.1% respectively).

The quantitative effects of nTiO<sub>2</sub> exposure on relative abundance of different genera, could be better appreciated when data reported in Fig. 2A from nTiO<sub>2</sub>-exposed samples were normalized to control samples and expressed as % values (Fig. S1). Some genera, such as *Stenotrophomonas*, *Sulfitobacter*, *Aquibacter* and *Variovorax*, notably increased after treatment with an increment on their relative abundances ranging from +100% to over 200%. On the other hand, *Kistimonas*, *Shewanella*, *Vibrio* or *Psychrobium* showed a drop of their relative abundances close to –100%.

The overall changes in the bacterial community composition induced by nTiO<sub>2</sub> in hemolymph samples can be depicted in a heatmap of the most predominant bacterial genera (≥1% abundance) (Fig. 3). The figure clearly emphasizes the decrease in abundance for *Kistimonas*, *Shewanella*, *Vibrio* and *Psychrobium* after treatment to nTiO<sub>2</sub>, while other genera seem less impacted by nTiO<sub>2</sub>. Moreover, the heatmap

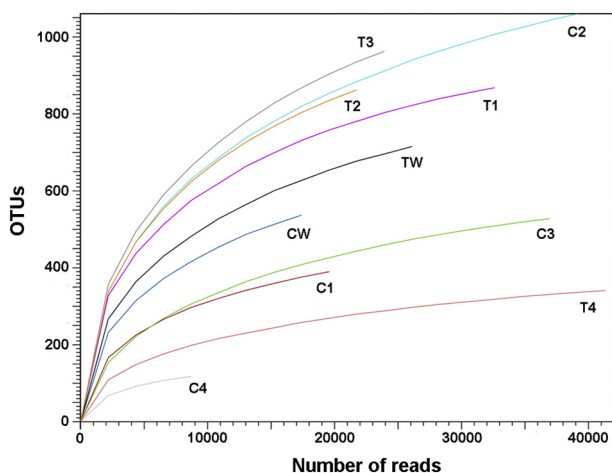


**Fig. 1.** Rarefaction curves for alpha-diversity metrics (number of total OTUs calculated from 16rDNA gene-based profiling analysis of the bacterial community) in water and hemolymph samples. CW = control seawater; TW = nTiO<sub>2</sub> treated seawater; C1–C4 = control mussels; T1–T4 = nTiO<sub>2</sub>-exposed mussels (n = 4).

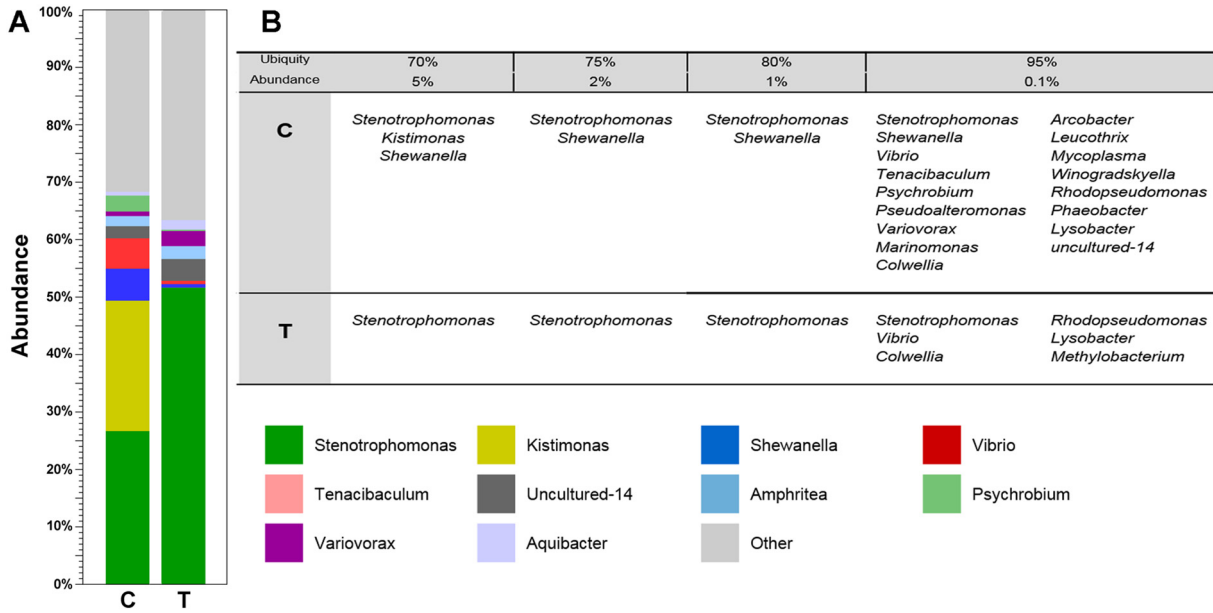


**Fig. 2.** Effect of nTiO<sub>2</sub> on the microbiome of *Mytilus galloprovincialis* hemolymph. A) Relative abundance of bacterial genera found in *Mytilus galloprovincialis* hemolymph by 16S rDNA gene-based profiling analysis. Data represent cumulative abundance, expressed in % of 4 replicates per condition. B) Core microbiome analysis for *Mytilus galloprovincialis* hemolymph microbiome analysed considering at different ubiquity and abundance thresholds. C = control mussels; T = nTiO<sub>2</sub>-exposed mussels.

highlighted the same trend among replicates despite the individual variations.

3.2.3. Microbiome analysis of exposure medium

The microbiota present in samples of ASW utilized for exposure experiment (control and nTiO<sub>2</sub>-exposed) was investigated and the results are reported in Fig. S2. A distinct composition of the overall bacterial community was observed compared to hemolymph samples. Interestingly, the genera *Stenotrophomonas* and *Kistimonas*, the main genera detected in hemolymph, were absent in all seawater samples (Fig. S2 A).

The microbiome profiles in samples of control and nTiO<sub>2</sub>-treated seawater were similar in composition, being mainly dominated by the genera *Shewanella*, *Vibrio*, *Tenacibaculum*, *Psychrobium* and *Marinomonas* (Fig. S2 B). However, a net decrease in abundance of *Shewanella* was observed in nTiO<sub>2</sub>-treated seawater with respect to

control water (from 47.9 to 26.2%) as well as of *Marinomonas* (from 6.3 to 3.3%) and *Psychrobium* (from 8.9 to 2.2%).

3.2.4. Principal coordinate analysis (PCoA)

A Principal Coordinates Analysis (PCoA) performed using Bray-Curtis distance matrices allowed to further analyse the factors responsible for differences among groups of samples. The analysis explained 82% of the total variation based on the three main ordines, clustering the samples in three characteristics groups. Fig. 4 shows a clear separation along the x-axis (PC1 = 48% of variability) between hemolymph of control and nTiO<sub>2</sub>-exposed samples. Only sample T4 appears separated from the other clusters showing an overall distinct diversity; however the main bacterial groups and the effect of the treatment in this sample appears to be similar to the other treated samples. Moreover, along the

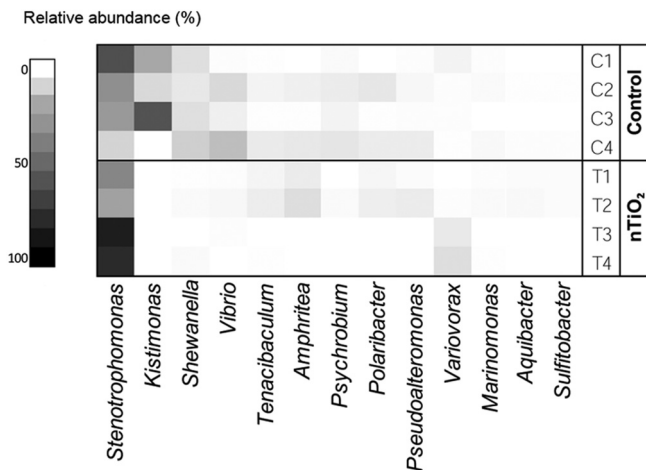


**Fig. 3.** Heatmap analysis of the microbial community at the genus level of *Mytilus galloprovincialis* hemolymph. Data represent only taxa with abundance >1% of total. C1–C4 = control mussels; T1–T4 = nTiO<sub>2</sub>-exposed mussels.

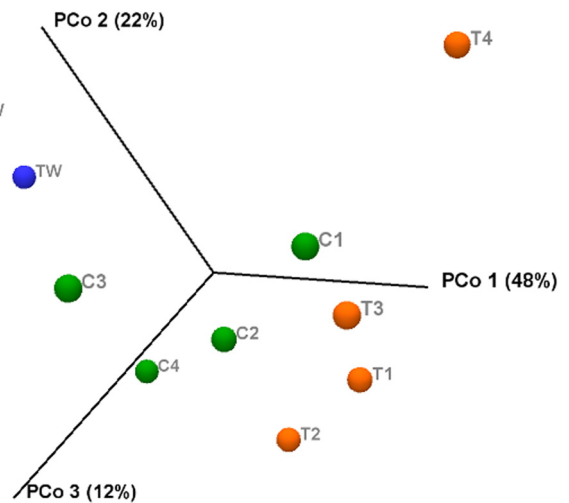


**Fig. 4.** 3D PCoA plots of beta diversity for seawater and *Mytilus galloprovincialis* hemolymph samples calculated using Principal coordinate Analysis (PCoA) applied on Bray-Curtis distance matrix. CW = control seawater; TW = nTiO<sub>2</sub> treated seawater; C1–C4 = control mussels; T1–T4 = nTiO<sub>2</sub>-exposed mussels.

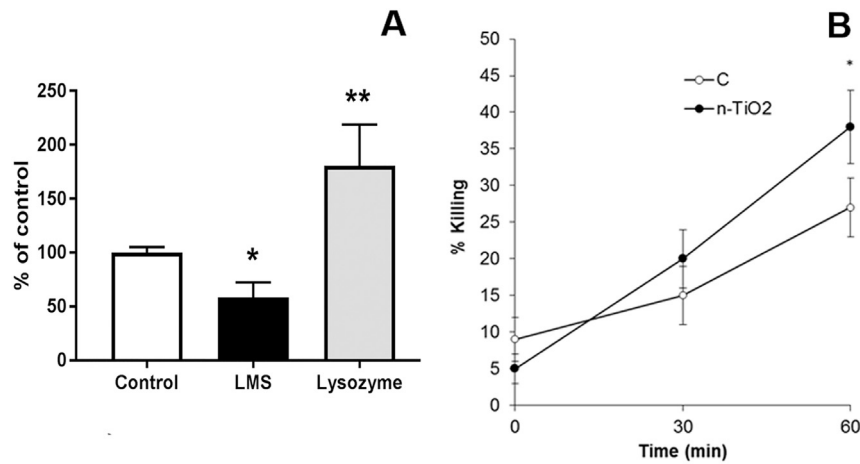


**Fig. 5.** Effects of nTiO<sub>2</sub> exposure (100 µg/L, 96 h) on *Mytilus galloprovincialis* functional immune parameters. A) Lysosomal membrane stability-LMS (grey bar) in hemocytes and lysozyme activity in hemolymph serum (black bar). Data are reported as mean % of control (N = 5) ± SD. \*P < 0.05, \*\*P < 0.01 (Mann-Whitney U test). B) In vitro bactericidal activity towards *E. coli* of whole hemolymph samples from control group (white dot) and nTiO<sub>2</sub> treated (black dot). Hemolymph was incubated with *E. coli* for 30 and 60 min as described in methods. Data, representing the mean of 4 experiments in triplicate, are expressed as percent of bacterial killing. \*P < 0.05, Mann-Whitney U test.

y-axis (PC2 = 22%) water samples are separated from hemolymph samples.

#### 4. Immune responses to nTiO<sub>2</sub> exposure

The effects of nTiO<sub>2</sub> exposure on *M. galloprovincialis* immune parameters (in hemocytes and hemolymph serum) have been thoroughly investigated in previous papers in same experimental conditions utilized in the present study (96 h exposure at a concentration of 100 µg/L/animal) (Barmo et al., 2013; Balbi et al., 2014). The results on the effects of functional and molecular immune parameters are summarized in Table S3.

To confirm the immunomodulatory effects of nTiO<sub>2</sub>, in the present study hemocyte LMS and lysozyme activity in hemolymph serum were evaluated, as the most simple and sensitive biomarkers of nTiO<sub>2</sub> exposure (Fig. 5). The results confirm the decrease in hemocyte LMS and increased serum lysozyme activity (Fig. 5A) induced by nTiO<sub>2</sub> observed in previous studies (Barmo et al., 2013; Balbi et al., 2014). Moreover, the overall bactericidal activity of mussel hemolymph was evaluated in whole hemolymph samples from control and nTiO<sub>2</sub> exposed mussels utilizing an in vitro bactericidal assay using *E. coli* as a model Gram (–) bacterium (Canesi et al., 2001). As shown in Fig. 5B, after 60 min incubation with *E. coli*, the hemolymph from nTiO<sub>2</sub>-exposed mussels showed a significantly higher percentage of bacterial killing (+60% with respect to controls; P < 0.05).

#### 5. Discussion

In the recent years, increasing attention has been given to the microbiome and its complex dynamics maintained within its host (human, animal, plant), as well as on the different factors that could affect their natural equilibrium (Flandroy et al., 2018). However, although invertebrate represents 95% of animal species, a minority of microbiome studies focus on this group. The interest in invertebrate-microbe interactions is also due to conservation of the mechanisms of innate immunity. Thus, understanding cross talk between microbes and invertebrate animals can lead to insights of broader relevance (Petersen and Osvatic, 2018). The results here obtained show that exposure to nTiO<sub>2</sub> resulted in a shift in the composition of microbial communities in the hemolymph of *M. galloprovincialis*. These represent the first data on the effects of NPs on the microbiome of a marine invertebrate, and suggest a possible relationship with the NP-induced immunomodulation.

Among invertebrates, increasing information is available on the microbiome of bivalve molluscs (oysters, clams, mussels), due not only to their ecological relevance, but also to their commercial importance as aquacultured species and susceptibility to increasing mortalities worldwide in relation to pathogenic microorganisms, bacteria in particular (Romero et al., 2014; Khan et al., 2018; King et al., 2018; Y.F. Li et al., 2018; Milan et al., 2018). To date, only one study is available in the mussel *Mytilus galloprovincialis*, the most important species reared in the Mediterranean and in the Galician coast (NW Spain). Vezzulli et al. (2017) reported data on hemolymph and digestive gland microbiome of mussels in comparison with the oyster *Crassostrea gigas* cultivated in the same site of the Ligurian Sea (NW Mediterranean, Italy) in the summer period (August) focusing on changes of microbial community in relation to the depuration process (Vezzulli et al., 2017).

The results here obtained show that in *M. galloprovincialis* hemolymph of control mussels appeared dominated by four bacterial genera, with *Stenotrophomonas* and *Kistimonas* accounting for about 50% of the total abundance, followed by *Shewanella* and *Vibrio* (~5% each), and other genera present at smaller percentages (<1%). These genera include a large variety of species that can be isolated from several aquatic organisms, bivalves in particular (Choi et al., 2010; Lee et al., 2012; King et al., 2018; Vezzulli et al., 2017). *Stenotrophomonas*, that was dominant in all samples, comprises bacteria of low virulence found in aquatic environments, previously observed in association with bivalves (Chauhan et al., 2013; Vezzulli et al., 2017). *Shewanella* includes some species involved in biofilm formation (Maurer-Jones et al., 2013; Qiu et al., 2017). To the genus *Vibrio* belong a variety of human and bivalve pathogens whose presence and interactions with bivalves is well documented (reviewed in Romalde et al., 2014; Balboa et al., 2016; Canesi and Pruzzo, 2016).

The results indicate a microbiota composition distinct from that previously identified in depurated mussels from the same area, where the hemolymph was dominated by *Vibrio* (56%) with smaller percentages of *Pseudoalteromonas* (9%), *Shewanella* (~7%) and *Amphritea* (~5%) (Vezzulli et al., 2017). The differences observed between the two studies could be mainly ascribed to the different sampling season and different experimental conditions. The present work was carried out in autumn (November), in order to reduce season-related stressful conditions for mussels, due to temperature related growth of pathogenic vibrios (Romero et al., 2014) or to peak in gametogenesis and spawning (Balbi et al., 2017). Moreover, after depuration, mussels were first acclimated in the lab in clean ASW for 24 h, and further kept in ASW for 4 days in the absence or

presence of added nTiO<sub>2</sub>, with daily changes in ASW medium. These conditions would allow for further changes in hemolymph microbial composition.

However, although the two studies are not fully comparable, the results can give an insight on the components of resident and the transient community of the mussel hemolymph microbiota. The relative abundance of *Shewanella* was similar in mussel sampled in November (this work) and August (Vezzulli et al., 2017), suggesting a certain stability, irrespectively of season and experimental conditions. In contrast, the main genera present in autumn samples, *Stenotrophomonas* and *Kistimonas* (this work) were not detected in summer (Vezzulli et al., 2017). Moreover, the *Vibrio* dominance, characteristic of the summer season, was lost in autumn, in line with the knowledge that *Vibrio* spread and establishment within bivalve tissues is favored by higher temperatures (Pruzzo et al., 2005; Romero et al., 2014). Environmental factors can shape or affect the dynamic and composition of microbiota within its host: the microbiome of marine invertebrates varies according to geographical scale or habitats (Ainsworth et al., 2015), and seasonal changes (Pierce et al., 2015), temperature in particular (Lokmer and Mathias Wegner, 2015). Further work is needed to fully appreciate seasonal shift of microbial population in *M. galloprovincialis* and the potential factors involved.

The microbiota of hemolymph from both control and nTiO<sub>2</sub>-treated mussels revealed a similar core composition. However, mussel exposure to nTiO<sub>2</sub> induced a shift in abundance of different genera. In particular, bacterial diversity of the core microbiome was decreased after exposure to nTiO<sub>2</sub>, when comparing the same level of ubiquity. We observed the almost complete disappearance of the genus *Kistimonas* and the dramatic decrease in *Shewanella* and *Vibrio*. On the contrary, some genera were more abundant in nTiO<sub>2</sub>-exposed samples: the genus *Stenotrophomonas* was found in all samples at different thresholds of ubiquity and abundance considered, suggesting its uttermost dominance in hemolymph microbiota, independent of exposure conditions. However, a further increase in abundance was induced by nTiO<sub>2</sub> exposure. Moreover, other genera with <1% of total abundance in control samples, were more preponderant after exposure (see Fig. S1); these include *Variovorax*, *Aquibacter* and *Sulfitobacter*. These bacteria are natural inhabitants of the marine environment (Hameed et al., 2014; Kwak et al., 2014; Fukui et al., 2015; Peoples et al., 2018) except for *Variovorax* that was mostly found in soil. However, Sirisena et al. (2018) found that this genus was the most abundant taxon on groundwater systems, suggesting a larger ecological niche on this bacterium. Due to the limited knowledge on the role and interactions of these genera in the microbiota of marine organisms, especially in mussels, the consequences of their changes in abundances in responses to nTiO<sub>2</sub> exposure are at present difficult to explain. It is noteworthy that, despite the individual variations, common effects of nTiO<sub>2</sub> were observed in all replicate samples, as highlighted by the heatmap (Fig. 3). This effect was also depicted by the PCoA analysis, where the replicates were gathered in separated clusters, therefore indicating dissimilarity between control and nTiO<sub>2</sub> treated samples, thereby underlining the impact of nTiO<sub>2</sub>.

With regards to available information on the effects of NP exposure in aquatic organisms, evidence has been reported for the impact of feed diet of different types of NPs (Cu-NPs, Ag-NPs and chitosan Ag nanocomposites) on the gut microbiome of zebrafish (Merrifield et al., 2013; Udayangani et al., 2017). NP feeding has been shown to affect the gut microbiome also in model invertebrates. Ingestion of AgNP (20 nm; 450 µg/mL) by *Drosophila* larva led to a remarkable decrease in midgut microbiota diversity (Han et al., 2014). In the soil oligochaete *Enchytraeus crypticus*, polystyrene nano-beads (50–100 nm) induced body weight reduction and shifts in the microbiome (Zhu et al., 2018). In addition to environmental factors, it is accepted that some pollutants appeared to interact with the stability of bivalve microbiota (Milan et al., 2018). To date, the results

represent the first data on the impact of NPs on the microbiome of in marine organisms.

Addition of nTiO<sub>2</sub> also resulted in changes in the microbiota of exposure medium; however, since artificial seawater was utilized, the presence of bacteria is likely to result only from the biological activity of mussels both in control and nTiO<sub>2</sub>-added water samples. Although the same genera encountered in hemolymph were also found in seawater, a distinct distribution was observed: water samples were dominated by *Shewanella*, whereas two main genera present in hemolymph were absent (*Stenotrophomonas* and *Kistimonas*). Moreover, PCoA data show that seawater samples were grouped together but separately from hemolymph samples, thereby pointing out the limited direct effects of nTiO<sub>2</sub> on seawater microbiota.

The effects observed in both hemolymph and waters samples may be ascribed to the general antibacterial activity of nTiO<sub>2</sub>. However, high concentrations (g/L) are required to inhibit the growth of bacteria, including *E. coli* (Sharma, 2009). Moreover, nTiO<sub>2</sub> was shown to alter aquatic bacterial communities at hundreds µg/L or mg/L levels (Binh et al., 2014; Jomini et al., 2015; Londono et al., 2017). In our experimental conditions, the Ti content in exposure medium, measured by both ICP-MS and ICP-AES analyses, showed high variability (Balbi et al., 2014), reflecting the instability of the nTiO<sub>2</sub> suspension, due to agglomeration and subsequent sedimentation of nTiO<sub>2</sub> (Brunelli et al., 2013). Moreover, much lower concentrations of Ti were recorded with respect to nominal added concentrations, ranging from 5 and 1.9 µg/L, detected 2 h after addition and at the end of exposure, respectively (Balbi et al., 2014). Therefore, the concentrations of nTiO<sub>2</sub> in exposure medium seem to be too low to be responsible for its direct antibacterial activity, although this hypothesis cannot be ruled out. This is however highly unlikely in hemolymph samples, where the concentration of Ti was below levels of detection (LOD of Ti = 0.1 µg/g, not shown).

In this light, the shift in hemolymph microbiome composition induced by nTiO<sub>2</sub> exposure may be due to the interplay between hemolymph microbiota and activity of the immune system. Previous data showed that exposure to nTiO<sub>2</sub>, in the same experimental conditions of the present study, induced immunomodulatory effects in *Mytilus* (Barmo et al., 2013; Balbi et al., 2014). nTiO<sub>2</sub> affect functional immune parameters (lysosome, phagocytosis) and induced a stimulation of the extracellular mechanisms of immune defense (ROS, NO and lysozyme release) along with modulation of expression of immune-related genes in hemocytes, suggesting that exposure to nTiO<sub>2</sub> may result in a stimulation of the immune response. These data are further supported by the results obtained in the present work, showing that, in addition to decreased LMS and increased soluble lysozyme activity, nTiO<sub>2</sub> exposure resulted in a net increase of the overall bactericidal activity of whole hemolymph samples. This parameter does not represent a simple proxy of immunocompetence, as the phagocytic activity, but the only measurement that provides complete information on the overall capacity of the mussel immune system not only to engulf, but also to kill microorganisms. Although for the bactericidal assay *E. coli* was utilized as a model Gram (–), these results may partly explain the decrease in the relative abundance of some genera (*Kistimonas*, *Shewanella*, *Psychrobium* and *Vibrio*) observed in the hemolymph of nTiO<sub>2</sub>-exposed mussels.

These data support the hypothesis that also in invertebrates the crosstalk between the innate immune system and the microbiome goes far beyond the achievement of a balance between tolerance to commensal microorganisms and immunity to pathogens. On one hand, the innate immune system plays an important part in shaping the microbiota into configurations that can be tolerated by the host and are beneficial for its metabolic activities; on the other, the microbiota integrates into whole-organism physiology and influences multiple facets of homeostatic processes through its effects on the innate immune system (Thaiss et al., 2016). This complex, bilateral interaction has a crucial role not only in human health, but also in other mammals, amphibians, invertebrates and plants (Felix et al., 2018; Robertson et al., 2018). In this light, it has been proposed that overlapping compositions

and interconnected roles of microbes in human, animal and plant health should be considered within the broader context of terrestrial and aquatic microbial ecosystems that are challenged by human activities, including chemical contamination (Flandroy et al., 2018). Invertebrates lack adaptive immunity, and only rely on innate immunity for interactions with resident and invading microorganisms; further research is needed on the relationship between the microbiome and immune system of key invertebrate species. These studies will represent the basis for better understanding how exposure to both contaminants and natural stressors may shape the interactions between the microbiome and the immune system, and the consequent impact of human activities on the health of different ecosystems.

## Acknowledgements

This project has received funding from the European Union's Horizon 2020 research and innovation programme under the Marie Skłodowska-Curie grant agreement PANDORA N° 671881 and the EU project H2020 VIVALDI grant number N° 678589.

## Appendix A. Supplementary data

Supplementary data to this article can be found online at <https://doi.org/10.1016/j.scitotenv.2019.03.133>.

## References

- Ainsworth, T., Krause, L., Bridge, T., Torda, G., Raina, J.-B., Zakrzewski, M., Gates, R.D., Padilla-Gamiño, J.L., Spalding, H.L., Smith, C., Woolesey, E.S., Bourne, D.G., Bongaerts, P., Hoegh-Guldberg, O., Leggat, W., 2015. The coral core microbiome identifies rare bacterial taxa as ubiquitous endosymbionts. *ISME J.* 9, 2261–2274. <https://doi.org/10.1038/ismej.2015.39>.
- Ananpattarachai, J., Boonto, Y., Kajitvichyanukul, P., 2016. Visible light photocatalytic antibacterial activity of Ni-doped and N-doped TiO<sub>2</sub> on *Staphylococcus aureus* and *Escherichia coli* bacteria. *Environ. Sci. Pollut. Res.* 23, 4111–4119. <https://doi.org/10.1007/s11356-015-4775-1>.
- ASTM, 2004. Standard guide for conducting static acute toxicity tests starting with embryos of four species of saltwater bivalve molluscs. <https://doi.org/10.1520/E0724-98>.
- Balbi, T., Smerilli, A., Fabbri, R., Ciacci, C., Montagna, M., Grasselli, E., Brunelli, A., Pojana, G., Marcomini, A., Gallo, G., Canesi, L., 2014. Co-exposure to n-TiO<sub>2</sub> and Cd<sup>2+</sup> results in interactive effects on biomarker responses but not in increased toxicity in the marine bivalve *M. galloprovincialis*. *Sci. Total Environ.* 493, 355–364. <https://doi.org/10.1016/j.scitotenv.2014.05.146>.
- Balbi, T., Fabbri, R., Montagna, M., Camisassi, G., Canesi, L., 2017. Seasonal variability of different biomarkers in mussels (*Mytilus galloprovincialis*) farmed at different sites of the Gulf of La Spezia, Liguria sea, Italy. *Mar. Pollut. Bull.* 116, 348–356. <https://doi.org/10.1016/j.marpolbul.2017.01.035>.
- Balboa, S., Lasa, A., Gerpe, D., Dieguez, A.L., Romalde, J.L., 2016. In: Romalde, Jesus L. (Ed.), *Microbiota associated to clams and oysters: a key factor for culture success*, in: *Oysters and Clams: Cultivation, Habitat Threats and Ecological Impact*. Nova Science Publishers, Inc, pp. 39–66.
- Barmo, C., Ciacci, C., Canonico, B., Fabbri, R., Cortese, K., Balbi, T., Marcomini, A., Pojana, G., Gallo, G., Canesi, L., 2013. In vivo effects of n-TiO<sub>2</sub> on digestive gland and immune function of the marine bivalve *Mytilus galloprovincialis*. *Aquat. Toxicol.* 132–133, 9–18. <https://doi.org/10.1016/j.aquatox.2013.01.014>.
- Binh, C.T.T., Tong, T., Gaillard, J.-F., Gray, K.A., Kelly, J.J., 2014. Common freshwater bacteria vary in their responses to short-term exposure to nano-TiO<sub>2</sub>: freshwater bacteria vary in responses to nano-TiO<sub>2</sub>. *Environ. Toxicol. Chem.* 33, 317–327. <https://doi.org/10.1002/etc.2442>.
- Bourne, D.G., Morrow, K.M., Webster, N.S., 2016. Insights into the coral microbiome: underpinning the health and resilience of reef ecosystems. *Annu. Rev. Microbiol.* 70, 317–340. <https://doi.org/10.1146/annurev-micro-102215-095440>.
- Bouwmeester, H., van der Zande, M., Jepson, M.A., 2018. Effects of food-borne nanomaterials on gastrointestinal tissues and microbiota: effects of food-borne nanomaterials on gastrointestinal tissues. *Wiley Interdiscip. Rev. Nanomed. Nanobiotechnol.* 10, e1481. <https://doi.org/10.1002/wnan.1481>.
- Brugman, S., Ikeda-Ohtsubo, W., Braber, S., Folkerts, G., Pieterse, C.M.J., Bakker, P.A.H.M., 2018. A comparative review on microbiota manipulation: lessons from fish, plants, livestock, and human research. *Front. Nutr.* 5. <https://doi.org/10.3389/fnut.2018.00080>.
- Brunelli, A., Pojana, G., Callegaro, S., Marcomini, A., 2013. Agglomeration and sedimentation of titanium dioxide nanoparticles (n-TiO<sub>2</sub>) in synthetic and real waters. *J. Nanopart. Res.* 15. <https://doi.org/10.1007/s11051-013-1684-4>.
- Canesi, L., Corsi, I., 2016. Effects of nanomaterials on marine invertebrates. *Sci. Total Environ.* 565, 933–940. <https://doi.org/10.1016/j.scitotenv.2016.01.085>.
- Canesi, L., Procházková, P., 2013. In: Boraschi, D., Duschl, A. (Eds.), *The invertebrate immune system as a model for investigating the environmental impact of nanoparticles*, in: *Nanoparticles and the Immune System*. Academic Press, Oxford, pp. 91–112.
- Canesi, L., Pruzzo, C., 2016. Specificity of innate immunity in bivalves: a lesson from bacteria, in: *Lessons in Immunity: From Single-Cell Organisms to Mammals*. L. Ballarín, M. Cammarata (Eds.). Academic Press, Elsevier Inc, pp. 79–88.
- Canesi, L., Pruzzo, C., Tarsi, R., Gallo, G., 2001. Surface interactions between *Escherichia coli* and hemocytes of the Mediterranean mussel *Mytilus galloprovincialis* Lam. leading to efficient bacterial clearance. *Appl. Environ. Microbiol.* 67, 464–468. <https://doi.org/10.1128/AEM.67.1.464-468.2001>.
- Canesi, L., Fabbri, R., Gallo, G., Vallotto, D., Marcomini, A., Pojana, G., 2010. Biomarkers in *Mytilus galloprovincialis* exposed to suspensions of selected nanoparticles (Nano carbon black, C60 fullerene, Nano-TiO<sub>2</sub>, Nano-SiO<sub>2</sub>). *Aquat. Toxicol.* 100, 168–177. <https://doi.org/10.1016/j.aquatox.2010.04.009>.
- Canesi, L., Frenzilli, G., Balbi, T., Bernardeschi, M., Ciacci, C., Corsolini, S., Della Torre, C., Fabbri, R., Faleri, C., Focardi, S., Guidi, P., Kočan, A., Marcomini, A., Mariottini, M., Nigro, M., Pozo-Gallardo, K., Rocco, L., Scarcelli, V., Smerilli, A., Corsi, I., 2014. Interactive effects of n-TiO<sub>2</sub> and 2,3,7,8-TCDD on the marine bivalve *Mytilus galloprovincialis*. *Aquat. Toxicol.* 153, 53–65. <https://doi.org/10.1016/j.aquatox.2013.11.002>.
- Canesi, L., Ciacci, C., Balbi, T., 2016. Invertebrate models for investigating the impact of nanomaterials on innate immunity: the example of the marine mussel *Mytilus* spp. *Curr. Bionanotechnol.* 2, 77–83. <https://doi.org/10.2174/2213529402666160601102529>.
- Chauhan, A., Green, S., Pathak, A., Thomas, J., Venkatraman, R., 2013. Whole-genome sequences of five oyster-associated bacteria show potential for crude oil hydrocarbon degradation. *Genome Announc.* 1. <https://doi.org/10.1128/genomeA.00802-13>.
- Chen, L., Guo, Y., Hu, C., Lam, P.K.S., Lam, J.C.W., Zhou, B., 2018. Dysbiosis of gut microbiota by chronic coexposure to titanium dioxide nanoparticles and bisphenol A: implications for host health in zebrafish. *Environ. Pollut.* 234, 307–317. <https://doi.org/10.1016/j.envpol.2017.11.074>.
- Choi, E.J., Kwon, H.C., Sohn, Y.C., Yang, H.O., 2010. *Kistimonas asteriae* gen. nov., sp. nov., a gammaproteobacterium isolated from *Asterias amurensis*. *Int. J. Syst. Evol. Microbiol.* 60, 938–943. <https://doi.org/10.1099/ijs.0.014282-0>.
- Ciacci, C., Canonico, B., Bilaničová, D., Fabbri, R., Cortese, K., Gallo, G., Marcomini, A., Pojana, G., Canesi, L., 2012. Immunomodulation by different types of N-oxides in the hemocytes of the marine bivalve *Mytilus galloprovincialis*. *PLoS One* 7, e36937. <https://doi.org/10.1371/journal.pone.0036937>.
- Corsi, I., Cherr, G.N., Lenihan, H.S., Labille, J., Hasselöf, M., Canesi, L., Dondero, F., Frenzilli, G., Hristozov, D., Punes, V., Della Torre, C., Pinsino, A., Libralato, G., Marcomini, A., Sabbioni, E., Matranga, V., 2014. Common strategies and technologies for the ecotoxicity assessment and design of nanomaterials entering the marine environment. *ACS Nano* 8, 9694–9709. <https://doi.org/10.1021/nn504684k>.
- de Lorgeril, J., Lucasson, A., Petton, B., Toulza, E., Montagnani, C., Clerissi, C., Vidal-Dupiol, J., Chaparro, C., Galinier, R., Escoubas, J.-M., Haffner, P., Dégremont, L., Charrière, G.M., Lafont, M., Delort, A., Vergnes, A., Chiarello, M., Faury, N., Rubio, T., Leroy, M.A., Péronig, A., Régler, D., Morga, B., Alunno-Bruscia, M., Boudry, P., Le Roux, F., Destoumieux-Garzon, D., Gueguen, Y., Mitta, G., 2018. Immune-suppression by OSHV-1 viral infection causes fatal bacteraemia in Pacific oysters. *Nat. Commun.* 9. <https://doi.org/10.1038/s41467-018-06659-3>.
- Defer, D., Desriac, F., Henry, J., Bourgougnon, N., Baudy-Floc'h, M., Brillet, B., Le Chevalier, P., Fleury, Y., 2013. Antimicrobial peptides in oyster hemolymph: the bacterial connection. *Fish Shellfish Immunol.* 34, 1439–1447. <https://doi.org/10.1016/j.fsi.2013.03.357>.
- Della Torre, C., Balbi, T., Grassi, G., Frenzilli, G., Bernardeschi, M., Smerilli, A., Guidi, P., Canesi, L., Nigro, M., Monaci, F., Scarcelli, V., Rocco, L., Focardi, S., Monopoli, M., Corsi, I., 2015. Titanium dioxide nanoparticles modulate the toxicological response to cadmium in the gills of *Mytilus galloprovincialis*. *J. Hazard. Mater.* 297, 92–100. <https://doi.org/10.1016/j.jhazmat.2015.04.072>.
- Desriac, F., Le Chevalier, P., Brillet, B., Leguerinel, I., Thuillier, B., Paillard, C., Fleury, Y., 2014. Exploring the hologenome concept in marine bivalvia: haemolymph microbiota as a pertinent source of probiotics for aquaculture. *FEMS Microbiol. Lett.* 350, 107–116. <https://doi.org/10.1111/1574-6968.12308>.
- Doyle, J.J., Ward, J.E., Mason, R., 2015. An examination of the ingestion, bioaccumulation, and depuration of titanium dioxide nanoparticles by the blue mussel (*Mytilus edulis*) and the eastern oyster (*Crassostrea virginica*). *Mar. Environ. Res.* 110, 45–52. <https://doi.org/10.1016/j.marenvres.2015.07.020>.
- Dudefoi, W., Moniz, K., Allen-Vercos, E., Ropers, M.-H., Walker, V.K., 2017. Impact of food grade and nano-TiO<sub>2</sub> particles on a human intestinal community. *Food Chem. Toxicol.* 106, 242–249. <https://doi.org/10.1016/j.fct.2017.05.050>.
- EFSA Panel on Food Additives and Nutrient Sources added to Food, 2016. Scientific opinion on the re-evaluation of titanium dioxide (E 171) as a food additive. *EFSA Journal* 2016;14(9):4545, 83 pp. doi:10.2903/j.efsa.2016.4545, n.d.
- Felix, K.M., Tahsin, S., Wu, H.-J.J., 2018. Host-microbiota interplay in mediating immune disorders: role of microbiota in immune disorders. *Ann. N. Y. Acad. Sci.* 1417, 57–70. <https://doi.org/10.1111/nyas.13508>.
- Flandroy, L., Poutahidis, T., Berg, G., Clarke, G., Dao, M.-C., Decaestecker, E., Furman, E., Haahtela, T., Massart, S., Plovier, H., Sanz, Y., Rook, G., 2018. The impact of human activities and lifestyles on the interlinked microbiota and health of humans and of ecosystems. *Sci. Total Environ.* 627, 1018–1038. <https://doi.org/10.1016/j.scitotenv.2018.01.288>.
- Foster, H.A., Ditta, I.B., Varghese, S., Steele, A., 2011. Photocatalytic disinfection using titanium dioxide: spectrum and mechanism of antimicrobial activity. *Appl. Microbiol. Biotechnol.* 90, 1847–1868. <https://doi.org/10.1007/s00253-011-3213-7>.

- Fukui, Y., Abe, M., Kobayashi, M., Satomi, M., 2015. *Sulfitobacter pacificus* sp. nov., isolated from the red alga *Pyropia yezoensis*. *Antonie Van Leeuwenhoek* 107, 1155–1163. <https://doi.org/10.1007/s10482-015-0407-5>.
- Gottschalk, F., Lassen, C., Kjoelholst, J., Christensen, F., Nowack, B., 2015. Modeling flows and concentrations of nine engineered nanomaterials in the Danish environment. *Int. J. Environ. Res. Public Health* 12, 5581–5602. <https://doi.org/10.3390/ijerph120505581>.
- Green, T.J., Siboni, N., King, W.L., Labbate, M., Seymour, J.R., Raftos, D., 2018. Simulated marine heat wave alters abundance and structure of *Vibrio* populations associated with the Pacific oyster resulting in a mass mortality event. *Microb. Ecol.* <https://doi.org/10.1007/s00248-018-1242-9>.
- Hameed, A., Shahina, M., Lin, S.-Y., Lai, W.-A., Hsu, Y.-H., Liu, Y.-C., Young, C.-C., 2014. *Aquibacter zeaxanthinifaciens* gen. nov., sp. nov., a zeaxanthin-producing bacterium of the family Flavobacteriaceae isolated from surface seawater, and emended descriptions of the genera *Aestuariibaculum* and *Gaetbulibacter*. *Int. J. Syst. Evol. Microbiol.* 64, 138–145. <https://doi.org/10.1099/ijs.0.052621-0>.
- Han, X., Geller, B., Moniz, K., Das, P., Chippindale, A.K., Walker, V.K., 2014. Monitoring the developmental impact of copper and silver nanoparticle exposure in *Drosophila* and their microbiomes. *Sci. Total Environ.* 487, 822–829. <https://doi.org/10.1016/j.scitotenv.2013.12.129>.
- Haynes, V.N., Ward, J.E., Russell, B.J., Agrios, A.G., 2017. Photocatalytic effects of titanium dioxide nanoparticles on aquatic organisms—current knowledge and suggestions for future research. *Aquat. Toxicol.* 185, 138–148. <https://doi.org/10.1016/j.aquatox.2017.02.012>.
- Ikeda-Ohtsubo, W., Brugman, S., Warden, C.H., Rebel, J.M.J., Folkerts, G., Pieterse, C.M.J., 2018. How can we define “optimal microbiota”? a comparative review of structure and functions of microbiota of animals, fish, and plants in agriculture. *Front. Nutr.* 5. <https://doi.org/10.3389/fnut.2018.00090>.
- Jomini, S., Clivot, H., Bauda, P., Pagnout, C., 2015. Impact of manufactured TiO<sub>2</sub> nanoparticles on planktonic and sessile bacterial communities. *Environ. Pollut.* 202, 196–204. <https://doi.org/10.1016/j.envpol.2015.03.022>.
- Khan, B., Clinton, S.M., Hamp, T.J., Oliver, J.D., Ringwood, A.H., 2018. Potential impacts of hypoxia and a warming ocean on oyster microbiomes. *Mar. Environ. Res.* 139, 27–34. <https://doi.org/10.1016/j.marenvres.2018.04.018>.
- King, W.L., Jenkins, C., Seymour, J.R., Labbate, M., 2018. Oyster disease in a changing environment: decrypting the link between pathogen, microbiome and environment. *Mar. Environ. Res.* <https://doi.org/10.1016/j.marenvres.2018.11.007>.
- Kwak, M.-J., Lee, J.-S., Lee, K.C., Kim, K.K., Eom, M.K., Kim, B.K., Kim, J.F., 2014. *Sulfitobacter geojensis* sp. nov., *Sulfitobacter noctilucae* sp. nov., and *Sulfitobacter noctiluicola* sp. nov., isolated from coastal seawater. *Int. J. Syst. Evol. Microbiol.* 64, 3760–3767. <https://doi.org/10.1099/ijs.0.065961-0>.
- Lee, J., Shin, N.-R., Lee, H.-W., Roh, S.W., Kim, M.-S., Kim, Y.-O., Bae, J.-W., 2012. *Kistimonas scapharcae* sp. nov., isolated from a dead ark clam (*Scapharca broughtonii*), and emended description of the genus *Kistimonas*. *Int. J. Syst. Evol. Microbiol.* 62, 2865–2869. <https://doi.org/10.1099/ijs.0.038422-0>.
- Li, K., Bihan, M., Methé, B.A., 2013. Analyses of the stability and core taxonomic memberships of the human microbiome. *PLoS One* 8, e63139. <https://doi.org/10.1371/journal.pone.0063139>.
- Li, J., Yang, S., Lei, R., Gu, W., Qin, Y., Ma, S., Chen, K., Chang, Y., Bai, X., Xia, S., Wu, C., Xing, G., 2018. Oral administration of rutile and anatase TiO<sub>2</sub> nanoparticles shifts mouse gut microbiota structure. *Nanoscale* 10, 7736–7745. <https://doi.org/10.1039/C8NR00386F>.
- Li, Y.-F., Yang, N., Liang, X., Yoshida, A., Osatomi, K., Power, D., Batista, F.M., Yang, J.-L., 2018. Elevated seawater temperatures decrease microbial diversity in the gut of *Mytilus coruscus*. *Front. Physiol.* 9. <https://doi.org/10.3389/fphys.2018.00839>.
- Lokmer, A., Mathias Wegner, K., 2015. Hemolymph microbiome of Pacific oysters in response to temperature, temperature stress and infection. *ISME J.* 9, 670–682. <https://doi.org/10.1038/ismej.2014.160>.
- Londono, N., Donovan, A.R., Shi, H., Geisler, M., Liang, Y., 2017. Impact of TiO<sub>2</sub> and ZnO nanoparticles on an aquatic microbial community: effect at environmentally relevant concentrations. *Nanotoxicology* 11, 1140–1156. <https://doi.org/10.1080/17435390.2017.1401141>.
- Mao, Z., Li, Y., Dong, T., Zhang, L., Zhang, Y., Li, S., Hu, H., Sun, C., Xia, Y., 2019. Exposure to titanium dioxide nanoparticles during pregnancy changed maternal gut microbiota and increased blood glucose of rat. *Nanoscale Res. Lett.* 14. <https://doi.org/10.1186/s11671-018-2834-5>.
- Maurer-Jones, M.A., Gunsolus, I.L., Meyer, B.M., Christenson, C.J., Haynes, C.L., 2013. Impact of TiO<sub>2</sub> nanoparticles on growth, biofilm formation, and Flavin secretion in *Shewanella oneidensis*. *Anal. Chem.* 85, 5810–5818. <https://doi.org/10.1021/ac400486u>.
- Menard, A., Drobne, D., Jemec, A., 2011. Ecotoxicity of nanosized TiO<sub>2</sub>. Review of *in vivo* data. *Environ. Pollut.* 159, 677–684. <https://doi.org/10.1016/j.envpol.2010.11.027>.
- Merrifield, D.L., Shaw, B.J., Harper, G.M., Saoud, I.P., Davies, S.J., Handy, R.D., Henry, T.B., 2013. Ingestion of metal-nanoparticle contaminated food disrupts endogenous microbiota in zebrafish (*Danio rerio*). *Environ. Pollut.* 174, 157–163. <https://doi.org/10.1016/j.envpol.2012.11.017>.
- Milan, M., Carraro, L., Fariselli, P., Martino, M.E., Cavaliere, D., Vitali, F., Boffo, L., Patarnello, T., Bargelloni, L., Cardazzo, B., 2018. Microbiota and environmental stress: how pollution affects microbial communities in Manila clams. *Aquat. Toxicol.* 194, 195–207. <https://doi.org/10.1016/j.aquatox.2017.11.019>.
- Olson, J.B., Kellogg, C.A., 2010. Microbial ecology of corals, sponges, and algae in mesophotic coral environments: mesophotic microbial ecology. *FEMS Microbiol. Ecol.* 73, 17–30. <https://doi.org/10.1111/j.1574-6941.2010.00862.x>.
- Peoples, L.M., Donaldson, S., Osuntokun, O., Xia, Q., Nelson, A., Blanton, J., Allen, E.E., Church, M.J., Bartlett, D.H., 2018. Vertically distinct microbial communities in the Mariana and Kermadec trenches. *PLoS One* 13, e0195102. <https://doi.org/10.1371/journal.pone.0195102>.
- Permet, F., Lagarde, F., Jeannée, N., Daigle, G., Barret, J., Le Gall, P., Quere, C., D'orbecastel, E.R., 2014. Spatial and temporal dynamics of mass mortalities in oysters is influenced by energetic reserves and food quality. *PLoS One* 9, e88469. <https://doi.org/10.1371/journal.pone.0088469>.
- Petersen, J.M., Osvatic, J., 2018. Microbiomes In Natura: importance of invertebrates in understanding the natural variety of animal-microbe interactions. *mSystems* 3. doi: <https://doi.org/10.1128/mSystems.00179-17>.
- Pflughoeft, K.J., Versalovic, J., 2012. Human microbiome in health and disease. *Annu. Rev. Pathol. Mech. Dis.* 7, 99–122. <https://doi.org/10.1146/annurev-pathol-011811-132421>.
- Pierce, M.L., Ward, J.E., 2018. Microbial ecology of the Bivalvia, with an emphasis on the family Ostreidae. *J. Shellfish Res.* 37, 793–806. <https://doi.org/10.2983/035.037.0410>.
- Pierce, M.L., Ward, J.E., Holohan, B.A., Zhao, X., Hicks, R.E., 2015. The influence of site and season on the gut and pallial fluid microbial communities of the eastern oyster, *Crassostrea virginica* (Bivalvia, Ostreidae): community-level physiological profiling and genetic structure. *Hydrobiologia* 765, 97–113. <https://doi.org/10.1007/s10750-015-2405-z>.
- Pietroliusti, A., Magrini, A., Campagnolo, L., 2016. New frontiers in nanotoxicology: gut microbiota/microbiome-mediated effects of engineered nanomaterials. *Toxicol. Appl. Pharmacol.* 299, 90–95. <https://doi.org/10.1016/j.taap.2015.12.017>.
- Pita, L., Rix, L., Slaby, B.M., Franke, A., Hentschel, U., 2018. The sponge holobiont in a changing ocean: from microbes to ecosystems. *Microbiome* 6. <https://doi.org/10.1186/s40168-018-0428-1>.
- Pruzzo, C., Gallo, G., Canesi, L., 2005. Persistence of vibrios in marine bivalves: the role of interactions with haemolymph components: *Vibrio* interactions with marine bivalve haemolymph. *Environ. Microbiol.* 7, 761–772. <https://doi.org/10.1111/j.1462-2920.2005.00792.x>.
- Qiu, T.A., Meyer, B.M., Christenson, K.G., Klaper, R.D., Haynes, C.L., 2017. A mechanistic study of TiO<sub>2</sub> nanoparticle toxicity on *Shewanella oneidensis* MR-1 with UV-containing simulated solar irradiation: bacterial growth, riboflavin secretion, and gene expression. *Chemosphere* 168, 1158–1168. <https://doi.org/10.1016/j.chemosphere.2016.10.085>.
- Robertson, S.J., Goethel, A., Girardin, S.E., Philpott, D.J., 2018. Innate immune influences on the gut microbiome: lessons from mouse models. *Trends Immunol.* 39, 992–1004. <https://doi.org/10.1016/j.it.2018.10.004>.
- Robichaud, C.O., Uyar, A.E., Darby, M.R., Zucker, L.G., Wiesner, M.R., 2009. Estimates of upper bounds and trends in nano-TiO<sub>2</sub> production as a basis for exposure assessment. *Environ. Sci. Technol.* 43, 4227–4233. <https://doi.org/10.1021/es8032549>.
- Romalde, J.L., Dieguez, A.L., Lasa, A., Balboa, S., 2014. New *Vibrio* species associated to molluscan microbiota: a review. *Front. Microbiol.* 4. <https://doi.org/10.3389/fmicb.2013.00413>.
- Romero, A., Costa, M., Forn-Cuni, G., Balseiro, P., Chamorro, R., Dios, S., Figueras, A., Novoa, B., 2014. Occurrence, seasonality and infectivity of *Vibrio* strains in natural populations of mussels *Mytilus galloprovincialis*. *Dis. Aquat. Org.* 108, 149–163. <https://doi.org/10.3354/dao02701>.
- Sharma, V.K., 2009. Aggregation and toxicity of titanium dioxide nanoparticles in aquatic environment—a review. *J. Environ. Sci. Health Part A* 44, 1485–1495. <https://doi.org/10.1080/10934520903263231>.
- Shreiner, A.B., Kao, J.Y., Young, V.B., 2015. The gut microbiome in health and in disease. *Curr. Opin. Gastroenterol.* 31, 69–75. <https://doi.org/10.1097/MOG.0000000000000139>.
- Sirisena, K.A., Daughney, C.J., Moreau, M., Sim, D.A., Lee, C.K., Cary, S.C., Ryan, K.G., Chambers, G.K., 2018. Bacterial bioclusters relate to hydrochemistry in New Zealand groundwater. *FEMS Microbiol. Ecol.* 94. <https://doi.org/10.1093/femsec/fy170>.
- Thaiss, C.A., Levy, M., Korem, T., Dohnalová, L., Shapiro, H., Jaitin, D.A., David, E., Winter, D.R., Gury-BenAri, M., Tatirovsky, E., Tuganbaev, T., Federici, S., Zmora, N., Zeevi, D., Dori-Bachash, M., Pevsner-Fischer, M., Kartvelishvili, E., Brandis, A., Harmelin, A., Shibolet, O., Halpern, Z., Honda, K., Amit, I., Segal, E., Elinav, E., 2016. Microbiota diurnal rhythmicity programs host transcriptome oscillations. *Cell* 167, 1495–1510.e12. <https://doi.org/10.1016/j.cell.2016.11.003>.
- Udayangani, R.M.C., Dananjaya, S.H.S., Nikapitiya, C., Heo, G.-J., Lee, J., De Zoysa, M., 2017. Metagenomics analysis of gut microbiota and immune modulation in zebrafish (*Danio rerio*) fed chitosan silver nanocomposites. *Fish Shellfish Immunol.* 66, 173–184. <https://doi.org/10.1016/j.fsi.2017.05.018>.
- Vezzulli, L., Stagnaro, L., Grande, C., Tassistro, G., Canesi, L., Pruzzo, C., 2017. Comparative 16S rDNA gene-based microbiota profiles of the Pacific oyster (*Crassostrea gigas*) and the Mediterranean mussel (*Mytilus galloprovincialis*) from a shellfish farm (Ligurian Sea, Italy). *Microb. Ecol.* 75, 495–504. <https://doi.org/10.1007/s00248-017-1051-6>.
- Vimbela, G., Ngo, S.M., Frazee, C., Yang, L., Stout, D.A., 2017. Antibacterial properties and toxicity from metallic nanomaterials. *Int. J. Nanomedicine Volume* 12, 3941–3965. <https://doi.org/10.2147/IJN.S134526>.
- Wendling, C.C., Goehlich, H., Roth, O., 2014. The structure of temperate phage-bacteria infection networks changes with the phylogenetic distance of the host bacteria. *Biol. Lett.* 14, 20180320. <https://doi.org/10.1098/rsbl.2018.0320>.
- Zhu, B.-K., Fang, Y.-M., Zhu, D., Christie, P., Ke, X., Zhu, Y.-G., 2018. Exposure to nanoplastics disturbs the gut microbiome in the soil oligochaete *Enchytraeus crypticus*. *Environ. Pollut.* 239, 408–415. <https://doi.org/10.1016/j.envpol.2018.04.017>.